ACCOUNTS
of chemical research

Paramagnetic Metal Ions in Pulsed ESR Distance Distribution Measurements

MING JI,[†] SHARON RUTHSTEIN,[†,‡] AND SUNIL SAXENA[†,*]

[†]*Department of Chemistry, University of Pittsburgh, Pittsburgh, Pennsylvania 15260, United States, and* [‡]*Department of Chemistry, Faculty of Exact Science, Bar Ilan University, Ramat-Gan 5290002, Israel*

RECEIVED ON OCTOBER 10, 2013

CONSPECTUS

The use of pulsed electron spin resonance (ESR) to measure interspin distance distributions has advanced biophysical research. The three major techniques that use pulsed ESR are relaxation rate based distance measurements, double quantum coherence (DQC), and double electron electron resonance (DEER). Among these methods, the DEER technique has become particularly popular largely because it is easy to implement on commercial instruments and because programs are available to analyze experimental data.

Researchers have widely used DEER to measure the structure and conformational dynamics of molecules labeled with the methanethiosulfonate spin label (MTSSL). Recently, researchers have exploited endogenously bound paramagnetic metal ions as spin probes as a way to determine structural constraints in metalloproteins. In this context Cu^{2+} has served as a useful paramagnetic metal probe at X-band for DEER based distance measurements. Sample preparation is simple, and a coordinated-Cu^{2+} ion offers limited spatial flexibility, making it an attractive probe for DEER experiments.

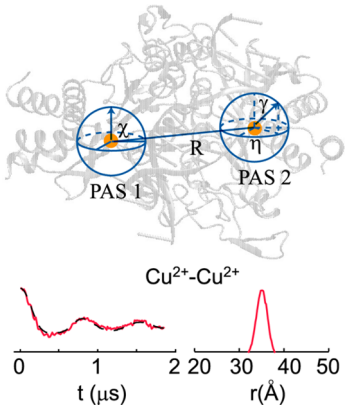

On the other hand, Cu^{2+} has a broad absorption ESR spectrum at low temperature, which leads to two potential complications. First, the Cu^{2+}-based DEER time domain data has lower signal to noise ratio compared with MTSSL. Second, accurate distance distribution analysis often requires high-quality experimental data at different external magnetic fields or with different frequency offsets.

In this Account, we summarize characteristics of Cu^{2+}-based DEER distance distribution measurements and data analysis methods. We highlight a novel application of such measurements in a protein–DNA complex to identify the metal ion binding site and to elucidate its chemical mechanism of function. We also survey the progress of research on other metal ions in high frequency DEER experiments.

1. Introduction

Advances in measurement of interspin distance distributions using pulsed electron spin resonance (ESR) have added an important new tool in biophysical research. There are three major pulsed ESR techniques for the distance distribution measurements with long-range distance accessibility: relaxation rate based distance distribution measurements,[1] double quantum coherence (DQC),[2,3] and double electron electron resonance (DEER) also known as pulsed electron double resonance (PELDOR).[4−8] Among these methods, the DEER/PELDOR technique has become the most widely used approach. The prevalence of DEER is largely due to the ease of implementation on commercial instruments, as well as due to the availability of programs that can analyze experimental data to obtain distance distributions.[9,10] However, microwave pulses at two different frequencies are required in DEER experiments.[4−8]

Most DEER distance distribution measurements are based on the site-directed spin-labeling technique wherein a cysteine residue is chemically modified with the nitroxide methanethiosulfonate spin label (MTSSL).[11] The application of site-directed spin-labeling and DEER in biophysics and materials research has been extensively reviewed recently.[12−15]

Figure 1 shows the R1 side chain generated by the reaction between cysteine(s) and MTSSL. The conformation of the side chain is defined by the dihedral angles of the five rotatable bonds between the protein backbone and the nitroxide ring (Figure 1), denoted as χ_1 through χ_5. One limitation of MTSSL is that the distance distributions are

Published on the Web 12/02/2013 www.pubs.acs.org/accounts
10.1021/ar400245z

often dominated by the conformational preferences of the R1 side chain. Numerous attempts have been made to account for the spatial distribution of R1 in experimental distance distributions.[16−23]

As an alternative, researchers have begun to employ endogenously bound paramagnetic metal ions as spin probes for ESR distance distribution measurements. Metal ions are involved in a variety of important biological processes, including photosynthetic electron transfer,[24,25] catalysis and gene regulation,[26,27] metabolism of carbon, nitrogen, and sulfur,[28] hydrolysis of amides and esters,[29−31] and disease mechanisms.[32−36] More than 30% of proteins require metal ions for function.[37] Utilizing these endogenously bound paramagnetic metal ions as probes for ESR detection only causes minimal functional perturbation to molecules. Distance distributions based on such endogenously bound metal ions may potentially be related to backbone conformations with greater ease than MTSSL, which may simplify the interpretation of protein structure.

Huber and coauthors presented the very first work in detecting the distance distribution between two Cu^{2+} centers in the dimer azurin structure.[38] Subsequently, other groups have used Cu^{2+} as a spin probe to detect the conformation of linked porphyrins, polypeptides, and proteins.[39−44] Iron−sulfur clusters have also been introduced as spin probes for structural detection.[45−47] To achieve high sensitivity, Gd^{3+} as well as Mn^{2+} have been used as spin probes for high-frequency DEER experiments.[48−58] The Gd^{3+}-based DEER distance method has been reviewed recently.[59]

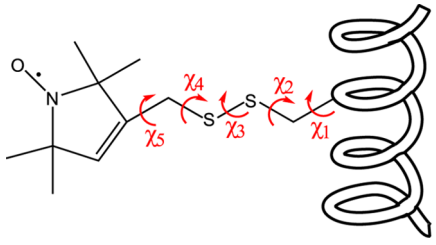

FIGURE 1. Structure of the R1 side chain. Five dihedral angles, $\chi_1-\chi_5$ are needed to describe the orientation of the side chain.

2. Challenges of Using Cu^{2+} in DEER Experiments

2.1. Sensitivity. The pulses in DEER experiments on Cu^{2+} excite fewer spins compared with MTSSL, which leads to a reduction in sensitivity of the DEER signal. Figure 2a shows the ESR absorption spectra of Cu^{2+} (red dotted line) and MTSSL (green solid line) at low temperature. Because of the larger anisotropic values of g and hyperfine tensors, the ESR absorption spectrum of Cu^{2+} is ~10 times broader than that of MTSSL at X-band (~9.5 GHz), as is shown in Figure 2a. The blue dashed line in Figure 2a shows the typical coverage of a 36 ns microwave pulse, which is typically used in DEER experiments. With the same pulse length, significantly fewer spins can be excited in Cu^{2+} spectrum compared with MTSSL.

The DEER time domain signal can be expressed as[5,13,43,61]

$$V(t) = 1 - \iint P(r)\left(\lambda - \lambda \cos\left[\frac{k}{r^3}(1 - 3\cos^2\theta)t\right]\right)\xi(\theta)\,\mathrm{d}\theta\,\mathrm{d}r \quad (1)$$

where $P(r)$ is the distance distribution and θ is the angle between the interspin vector and the external magnetic field, as shown in Figure 3a. k is a constant that is proportional to the product of the g values of two spin centers, and r is the distance between two spins. In eq 1, λ is the modulation depth and $\xi(\theta)$ is the geometrical factor. The broad Cu^{2+} ESR absorption spectrum at low temperature leads to a low modulation depth in DEER, as well as possible complications from limited excitation of spins. These are discussed in the following sections.

2.2. Modulation Depth. The modulation depth, λ, is the fraction of spins excited by the pump pulse, which are also coupled to the spins that are excited by the observer pulse.[62]

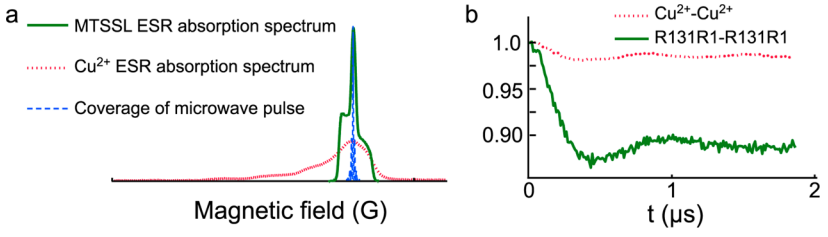

FIGURE 2. (a) ESR absorption spectra of Cu^{2+} (red dotted line) and MTSSL (green solid line). The coverage of a 36 ns microwave pulse is shown in blue dashed line; (b) $Cu^{2+}-Cu^{2+}$ (red dotted line)[44] and R131R1−R131R1 DEER (green solid line)[60] signals after baseline subtraction in the *Eco*RI−DNA complex with 44 and 48 ns pump pulse, respectively.

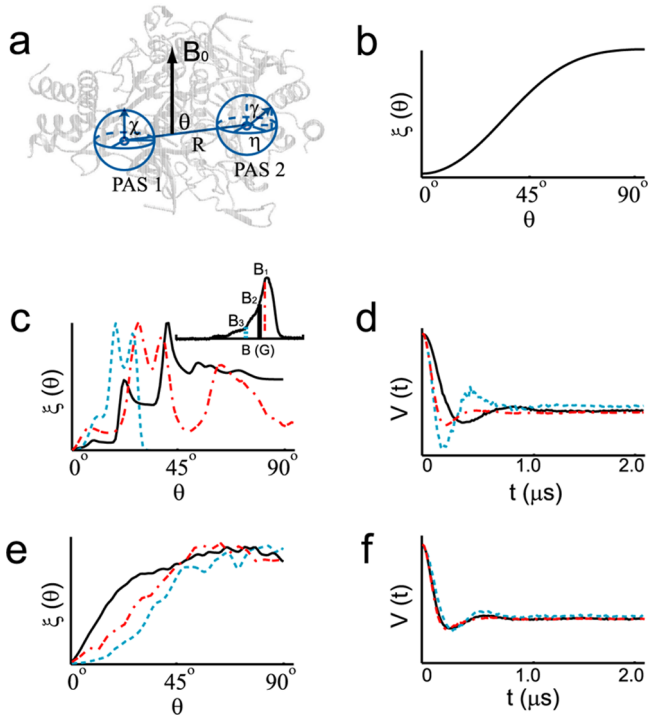

FIGURE 3. (a) The diagram shows the orientation, θ, of a vector connecting two interacting spins, R, with respect to the external magnetic field $\mathbf{B}_0$. The relative orientation of the two spin centers is defined by three angles χ, γ, and η. PAS1 and PAS2 denote the principle axis systems of the **g**-tensors of the first and second spin, respectively. (b) Ideal geometrical factor, $\xi(\theta)$. (c) Representative calculations of the geometrical factor $\xi(\theta)$ at three magnetic fields ($\mathbf{B}_1 = 3342$ G, $\mathbf{B}_2 = 3290$ G, and $\mathbf{B}_3 = 3060$G) shown in the inset. The simulations assume a small orientational distribution (standard deviation of 2°) between two Cu^{2+} centers. The pump pulse frequency is 92 MHz lower than the observer pulse frequency in these simulations. (d) Simulated DEER signals at three magnetic fields with the geometrical factors as shown in panel c. (e) The geometrical factor $\xi(\theta)$ at three magnetic fields as shown in Figure 3c inset ($\mathbf{B}_1 = 3342$ G, $\mathbf{B}_2 = 3290$ G, and $\mathbf{B}_3 = 3060$G) with a larger orientational distribution (standard deviation of 10°). (f) Simulated DEER signals at three magnetic fields with the geometrical factors shown in panel e.

The modulation depth depends on the pump pulse length as well as the shape of the ESR absorption spectrum.[4,63] A small modulation depth causes a low signal-to-noise ratio in the time domain data.[64,65] Also it is disadvantageous in the discrimination of nuclear modulations. Figure 2b shows the $Cu^{2+}-Cu^{2+}$ (red dotted line) and R131R1−R131R1 DEER time domain data (green solid line) in the specific *Eco*R-I−DNA complex. The $Cu^{2+}-Cu^{2+}$ DEER data with a shorter pump pulse (44 ns) has a much smaller modulation depth (∼2%) compared with the ∼13% modulation depth of R131R1−R131R1 with a longer pump pulse (48 ns).[44,60] By use of a commercially available microwave pulse forming unit to provide shorter pump pulses (e.g., 16 ns) and by choice of a proper frequency offset to minimize nuclear modulation, data with modulation depth of ∼12% can be obtained on Cu^{2+} at X-band (∼9.5 GHz).[65]

Interestingly, the six-pulse double quantum coherence (DQC)-based distance distribution measurements have a small background signal,[66] which allows for an easier extraction of the dipolar interaction. On the other hand, the DQC signal has substantial contributions from electron−nuclear interactions between the electron spin and neighboring ^{14}N, as well as ^{1}H, nuclear spins that are present in the amino acid coordination environment. These nuclear modulation effects may swamp the modulation due to the electron−electron dipolar interactions and make it difficult to measure the interspin distance distribution.

We recently presented a simple way to minimize these low-frequency nuclear peaks in the DQC spectrum and resolve the dipolar interaction between two Cu^{2+} centers with high sensitivity, by dividing two DQC signals with different pulse lengths.[66] This simple DQC method has a signal-to-noise ratio twice as high as DEER per shot. Further improvements in Cu^{2+} based DQC can be made by the use of narrower pulse lengths and by manipulating the pulse sequence to avoid acquisition of two DQC time domain signals. However, because of the narrower pulse lengths in the experiments, the power of the microwave pulse required in DQC is much higher than that in the DEER experiment. Additionally, the 256-step phase cycling in the experiment leads to a much longer data collection time. These factors limit the application of DQC on commercial instruments.

2.3. Orientational Selectivity Effect. In Cu^{2+}-based DEER, because of the broad absorption ESR spectrum, a typical microwave pulse of ∼36 ns can only excite a small portion of the θ angles. Both the electron−electron dipolar frequency [$\omega_{ee} = k/r^3(1 - 3\cos^2\theta)$], as well as the geometrical factor, $\xi(\theta)$, depend on the position of the microwave pulse. Hence, the DEER signals at different external magnetic field positions might have different modulation periods and modulation depths. This phenomenon is known as the "orientational selectivity" effect.[39,41,43,67,68]

In MTSSL-based DEER, the interplay of the anisotropies of g and hyperfine tensors and the flexibility of the R1 side chain typically randomize the relative orientation between the spin labels. When a pump pulse (e.g., 36 ns) is applied at the maximum of the MTSSL absorption spectrum, an ideal θ excitation profile [i.e., geometrical factor, $\xi(\theta)$] can be achieved as shown in Figure 3b.[41−43] In this case, the model-free Tikhonov regularization method has been developed to analyze the time domain data and obtain accurate distance distributions.[9,10]

In Cu^{2+}-based DEER, the signal may potentially depend on the relative orientation between the two metal ions. For the case of Cu^{2+}, the relative orientation between the two metal ions can be defined by three angles χ, γ, and η with certain orientational distribution, as shown in Figure 3a. Simulations with a pump pulse of 36 ns, shown in Figure 3c, yield three different geometrical factors at three different magnetic fields ($\mathbf{B}_1 = 3342$ G, $\mathbf{B}_2 = 3290$ G, and $\mathbf{B}_3 = 3060$ G). For these simulations, χ, γ, and η angles are 60°, 60° and 0°, respectively. Each angle is assumed to be Gaussian distributed with a standard deviation of 2°.

The simulated DEER time domain data shown in Figure 3d with geometrical factors from Figure 3c shows that even with the same distance distribution, this partial selectivity can potentially lead to different DEER signals[39,41−43,67,68] at different external magnetic field positions. Figure 3e shows that with the increase of the orientational distribution between two Cu^{2+} centers, the geometrical factors become broader and more θ angles are excited.[43] Accordingly, the time domain orientational selectivity effect is largely reduced as shown in Figure 3f.

DEER experiments on peptides and proteins show that the orientational selectivity effects are small but detectable.[43,44] The Cu^{2+}−Cu^{2+} DEER data in the *Eco*RI−DNA complex are shown in Figure 4a. The modulation periods changes by ∼60 ns (∼10% of the modulation period) at different magnetic fields.[44] Nevertheless, the data analyzed by using the model-free Tikhonov regularization method gives distance distributions that have artifacts (shoulder peaks) and most probable distances that differ by 1−3 Å (dashed lines shown in Figure 4b).[43] A difference in the width of the distance distributions may also be observed.[43] If only the most probable distances are needed and when the orientational selectivity effects are weak, the measured most probable distances based on Tikhonov regularization method are still acceptable within 1−3 Å error range.[40,43] For a more accurate measurement, one needs to collect data at different magnetic fields and frequency offsets and include the effects of orientational selectivity to analyze all the data.[43] As shown in Figure 4, a single distance distribution can fit the data when orientional selectivity is included in the analysis.[44] On smaller molecules, the data can also be analyzed based on molecular dynamics simulations and DFT calculations.[41,42,68] Strong suppression of orientational selectivity can also be achieved by summing experimental traces collected at different external magnetic fields (field averaging)[69,70] or with different frequency offsets.[71]

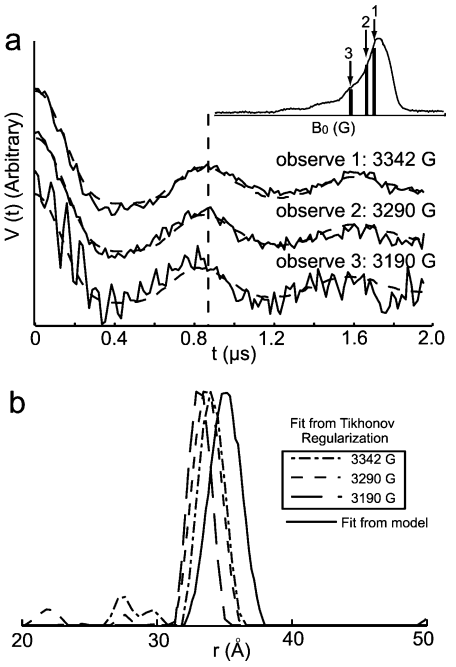

FIGURE 4. (a) Cu^{2+}−Cu^{2+} DEER signal in the *Eco*RI−DNA complex at different magnetic fields with the same frequency offset (100 MHz). The positions of the observer pulse are highlighted on the absorption ESR spectrum shown in the inset. The normalized signals are offset in the *y*-axis in order to clearly indicate the modulation periods. The vertical dashed line indicates the modulation period difference; the dashed line shows the simulations using the procedure described in ref 43. (b) The distance distribution functions (dashed lines) obtained at different external magnetic fields (3342, 3290, and 3190 G) using the Tikhonov regularization method; the Cu^{2+}−Cu^{2+} distance distribution (solid line) obtained by accounting for orientational selectivity.

3. Applications of Metal Ion-Based DEER

3.1. Elucidation of Protein−DNA Interaction by Cu^{2+}-Based DEER. We have recently focused on the use of ESR to examine the relationship between DNA sequence recognition and catalytic specificity in a DNA-modifying enzyme. The *Eco*RI endonuclease, a 62 kDa homodimer, recognizes the DNA site 5′-GAATTC-3′ and cleaves both DNA strands in the presence of the catalytic cofactor Mg^{2+}. Interestingly, the DNA cleavage rates are as much as 10^6-fold higher for the GAATTC site than for sites with a different base pair sequence. Importantly, Cu^{2+} by itself does not support DNA cleavage by *Eco*RI.[72] Therefore, it is appropriate as a spin probe in this protein−DNA system. Cu^{2+}-based distance measurements thus provide an exciting route to probe the structural and electrostatic effects that determine site specific catalysis in this class of enzymes.

We utilized bound Cu^{2+} ions and site-directed spin-labeling to shed light on the Cu^{2+} interaction with *Eco*RI. X-band pulsed techniques like electron spin echo envelope modulation (ESEEM) spectroscopy and hyperfine sublevel

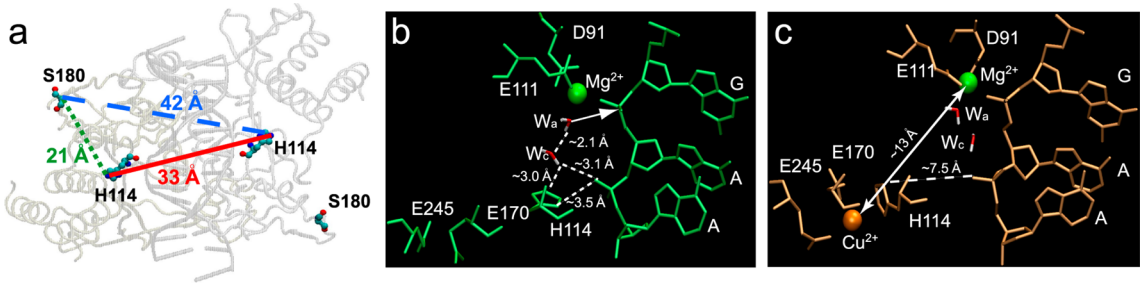

FIGURE 5. (a) The H114 N_ε–H114 N_ε (red solid line), as well as intra- (green dotted line) and intermonomer (blue dashed line) S180 C_α–H114 N_ε distances from crystal structure of metal-free *Eco*RI–DNA complex (PDB ID 1CKQ).[73] (b) The local structure of the *Eco*RI–DNA complex with only Mg^{2+}. (c) The local structure of the *Eco*RI–DNA complex with both Mg^{2+} and Cu^{2+}.

corelation (HYSCORE) spectroscopy results established that Cu^{2+} ions coordinate to a histidine in *Eco*RI. There are five histidine residues in each *Eco*RI monomer (H31, H114, H147, H162, H225). We obtained Cu^{2+}–Cu^{2+} (on wild-type *Eco*RI) and Cu^{2+}–S180R1 distances using DEER–ESR to identify the Cu^{2+}-coordinated histidine. Interestingly, more than one complete modulation period was observed for the Cu^{2+}–Cu^{2+} DEER data (Figure 4a). This observation indicates that the endogenously bound Cu^{2+} in the *Eco*RI–DNA complex provides a relatively fixed reference point for the distance measurements. This may be an advantage when two close distance distributions need to be resolved.

A single, most probable Cu^{2+}–Cu^{2+} distance distribution of 35 Å was observed with a standard deviation of 1 Å. Cu^{2+}–S180R1 distance measurements yielded two most probable distances at 22 and 42 Å with standard deviations of 2 and 3 Å, respectively. These distances were similar to the H114 N_ε–H114 N_ε distance (red solid line in Figure 5a), as well as H114 N_ε–S180 C_α intra- (green dotted line in Fiure 5a) and intermonomer (blue dashed line in Figure 5a) distances from the metal-free *Eco*RI–DNA crystal structure.[73] The distance distributions from ESR experiments were uniquely consistent with Cu^{2+} binding to H114. This was strongly supported by biochemical studies, which showed that the mutant H114Y–DNA complex binds Cu^{2+} with 1600-fold lower affinity than the wild-type *Eco*RI–DNA complex.

Unexpectedly, we found that Cu^{2+} is a powerful inhibitor of *Eco*RI catalysis; 100 μM Cu^{2+} completely inhibits cleavage by wild-type *Eco*RI. On the other hand, even at 200 μM, Cu^{2+} does not inhibit H114Y-catalyzed DNA cleavage in the presence of Mg^{2+}. This data further supports our conclusion that Cu^{2+} binds to H114 rather than the negative charge cluster (E111, D91, G**p**AATTC) that coordinates to Mg^{2+}.

An earlier model from Jen-Jacobson's group suggests that sequence-dependent DNA distortion has a critical function in *Eco*RI catalysis.[74] As shown in Figure 5b, the Mg^{2+}-bound water (W_a) that makes the nucleophilic attack on the scissile phosphate is precisely positioned by H-bonding to another water (named W_c). The W_c water is held in turn by H-bonding to both H114–Nε and a phosphoryl oxygen of the phosphate GA**p**ATTC, one step downstream from the scissile phoshate. This water network is only possible when *Eco*RI-induced DNA distortion creates a unique configuration, which brings the two phosphates into an unusual spatial relationship. Detailed MD simulations with explicit solvent showed that H114 is ~4 Å from its normal position in the presence of Cu^{2+} as shown in Figure 5c. Lacking interaction with H114, the GA**p**A phosphate moves to where it cannot support the water network that is crucial for the DNA cleavage. The overall picture is that the conformation essential for catalysis no longer exists in the presence of Cu^{2+}.

3.2. Selective Measurement of Cu^{2+}–Cu^{2+} Distances in a Multicopper Binding Protein. Recently, MacMillan and coworkers applied a new DEER technique to selectively measure Cu^{2+}–Cu^{2+} distance distributions in nitrite reductase from *Achromobacter xylosoxidans* (AxNiR).[75] Each monomer in this homotrimeric protein contains two different types of Cu^{2+} sites. The presence of six Cu^{2+} in the protein leads to overlapping distances that are not completely resolved in the DEER experiment. The authors were able to selectively measure distances between Cu^{2+} ions in one of the two sites by exploiting the differences in spin–lattice relaxation times. In this approach, an inversion recovery filter was used before the DEER sequence to suppress the signal from one of the two Cu^{2+} sites at a time.[75]

3.3. The Application of Other Metal Ions in DEER Experiments. High-quality DEER data using Gd^{3+} as a spin probe have been observed at high magnetic fields.[48−57] Gd^{3+} is a $S = 7/2$ ion with an isotropic **g**-factor. Several characters of Gd^{3+} make it a candidate for the DEER distance distribution measurements at high fields.[55] First, with the increase of frequency, the central transition $|-1/2\rangle \rightarrow |1/2\rangle$

narrows. Therefore, the sensitivity of Gd^{3+} in ESR increases with increasing of frequency. Second, because of the large zero-field-splitting distribution, the central transition can be considered effectively isotropic and Gd^{3+} abolishes the orientational selectivity effect at high magnetic fields. Thus, Gd^{3+}-based DEER allows the determination of precise distance distributions from DEER time domain traces by using the model-free Tikhonov regularization. The collection of a series of data at different external magnetic fields or with different frequency offsets is therefore not needed.[76] Furthermore, the use of cysteine-specific Gd^{3+} labels allows the application of Gd^{3+}-based DEER to any protein.[59] The Cu^{2+}-based DEER method can be similarly generalized by the use of EDTA–Cu^{2+} labels that can be incorporated into proteins through a disulfide linkage on cysteines.[77] Similar to Gd^{3+}, Mn^{2+} also displays an intense and relatively narrow center transition at high fields. On the other hand, the reduced toxicity of Mn^{2+} compared with Gd^{3+} makes the Mn^{2+}-based distance distribution measurements even more attractive at high fields.[58] There are also reports of DEER distance distribution measurements by using iron–sulfur clusters.[45] The electron spin delocalization over the cluster causes the point-dipole approximation to break down, and the spin projection factors need to be included to analyze data.[46,47]

4. Summary and Outlook

In this Account, we presented the application of paramagnetic metal ion Cu^{2+} in DEER. Although small modulation depth and orientational selectivity effects complicate the data collection and analysis procedures, the simple sample preparation process and limited spatial flexibility make Cu^{2+} an attractive probe for research. The application of Cu^{2+}-based distance measurements in the restriction endonuclease *Eco*RI–DNA complex illustrates the potential of using Cu^{2+} to probe structural and electrostatic effects that determine site specific catalysis in this class of enzymes. The development of methods that use other paramagnetic metal ions, for example, Gd^{3+} and Mn^{2+}, as spin probes for high-field DEER experiments may overcome the orientational selectivity effect from Cu^{2+}-based DEER and extend the reach of pulsed ESR distance distribution measurements.[48,58]

This research was supported by National Science Foundation Grants MCB 0842956 and MCB 1157712.

BIOGRAPHICAL INFORMATION

Ming Ji received his M.S. degree in Chemistry from Nanjing University in 2006. He is currently a graduate student at University of Pittsburgh.

Sharon Ruthstein received her Ph.D. from the Weizmann Institute in 2008 (with D. Goldfarb). She was a postdoctoral fellow at the University of Pittsburgh (with S. Saxena). She joined the Department of Chemistry at Bar-Ilan University in October 2011 as a senior lecturer. Her research is aimed at studying biological pathways in human and bacteria cells that involve metal ions, using pulsed EPR spectroscopy.

Sunil Saxena is a Professor of Chemistry at the University of Pittsburgh. His research interests focus on the development of electron spin resonance spectroscopy and its applications to biophysics, including protein–DNA interactions and metals in biology.

FOOTNOTES

*Correponding author. Phone: (412) 624-8680. Fax: (412) 624-8611. E-mail: sksaxena@pitt.edu.

The authors declare no competing financial interest.

REFERENCES

1 Eaton, S. S.; Eaton, G. R. In *Distance Measurements in Biological Systems by EPR*; Berliner, L. J., Eaton, S. S., Eaton, G. R., Eds.; Kluwer Academic/Plenum Publisher: New York, 2000; Vol. 19, pp 19–154.

2 Saxena, S.; Freed, J. H. Theory of double quantum two-dimensional electron spin resonance with application to distance measurements. *J. Chem. Phys.* **1997**, *107*, 1317–1340.

3 Borbat, P. P.; Freed, J. H. Multiple-quantum ESR and distance measurements. *Chem. Phys. Lett.* **1999**, *313*, 145–154.

4 Milov, A. D.; Ponomarev, A. B.; Tsvetkov, Y. D. Electron-electron double resonance in electron spin echo: Model biradical systems and the sensitized photolysis of decalin. *Chem. Phys. Lett.* **1984**, *110*, 67–72.

5 Larsen, R. G.; Singel, D. J. Double electron–electron resonance spin–echo modulation: Spectroscopic measurement of electron spin pair separations in orientationally disordered solids. *J. Chem. Phys.* **1993**, *98*, 5134–5146.

6 Milov, A. D.; Maryasov, A. G.; Tsvetkov, Y. D. Pulsed electron double resonance (PELDOR) and its applications in free-radical research. *Appl. Magn. Reson.* **1998**, *15*, 107–143.

7 Martin, R. E.; Pannier, M.; Diederich, F.; Gramlich, V.; Hubrich, M.; Spiess, H. W. Determination of end-to-end distances in a series of TEMPO diradicals of up to 2.8 nm length with a new four-pulse double electron electron resonance experiment. *Angew. Chem., Int. Ed. Engl.* **1998**, *37*, 2833–2837.

8 Pannier, M.; Veit, S.; Godt, A.; Jeschke, G.; Spiess, H. W. Dead-time free measurement of dipole–dipole interactions between electron spins. *J. Magn. Reson.* **2000**, *142*, 331–340.

9 Jeschke, G.; Panek, G.; Godt, A.; Bender, A.; Paulsen, H. Data analysis procedures for pulse ELDOR measurements of broad distance distributions. *Appl. Magn. Reson.* **2004**, *26*, 223–244.

10 Chiang, Y.-W.; Borbat, P. P.; Freed, J. H. The determination of pair distance distributions by pulsed ESR using Tikhonov regularization. *J. Magn. Reson.* **2005**, *172*, 279–295.

11 Hubbell, W. L.; Altenbach, C. Investigation of structure and dynamics in membrane proteins using site-directed spin labeling. *Curr. Opin. Struct. Biol.* **1994**, *4*, 566–573.

12 Steinhoff, H.-J. Inter- and intra-molecular distances determined by EPR spectroscopy and site-directed spin labeling reveal protein-protein and protein-oligonucleotide interaction. *Biol. Chem.* **2005**, *385*, 913–920.

13 Schiemanna, O.; Prisner, T. F. Long-range distance determinations in biomacromolecules by EPR spectroscopy. *Q. Rev. Biophys.* **2007**, *40*, 1–53.

14 Tsvetkov, Y. D.; Milov, A. D.; Maryasov, A. G. Pulsed electron-electron double resonance (PELDOR) as EPR spectroscopy in nanometer range. *Russ. Chem. Rev.* **2008**, *77*, 487–520.

15 Jeschke, G. DEER distance measurements on proteins. *Annu. Rev. Phys. Chem.* **2012**, *63*, 419–446.

16 Polyhach, Y.; Bordignon, E.; Jeschke, G. Rotamer libraries of spin labelled cysteines for protein studies. *Phys. Chem. Chem. Phys.* **2011**, *13*, 2356–2366.

17 Hatmal, M. M.; Li, Y.; Hegde, B. G.; Hegde, P. B.; Jao, C. C.; Langen, R.; Haworth, I. S. Computer modeling of nitroxide spin labels on proteins. *Biopolymers* **2011**, *97*, 35–44.

18 Klose, D.; Klare, J. P.; Grohmann, D.; Kay, C. W.; Werner, F.; Steinhoff, H. J. Simulation vs. reality: A comparison of in silico distance predictions with DEER and FRET measurements. *PLoS One* **2012**, *7*, No. e39492.

19 Hagelueken, G.; Ward, R.; Naismith, J. H.; Schiemann, O. MtsslWizard: In silico spin-labeling and generation of distance distributions in PyMOL. *Appl. Magn. Reson.* **2012**, *42*, 377–391.

20 Mamonov, A. B.; Lettieri, S.; Ding, Y.; Sarver, J. L.; Palli, R.; Cunningham, T. F.; Saxena, S.; Zuckerman, D. M. Tunable, mixed-resolution modeling using library-based Monte Carlo and graphics processing units. *J. Chem. Theory Comput.* **2012**, *8*, 2921–2929.

21 Sarver, J. L.; Townsend, J. E.; Rajapakse, G.; Jen-Jacobson, L.; Saxena, S. Simulating the dynamics and orientations of spin labeled side chains in a protein−DNA complex. *J. Phys. Chem. B* **2012**, *116*, 4024–4033.

22 Roux, B.; Islam, S. M. Restrained-ensemble molecular dynamics simulations based on distance histograms from double electron−electron resonance spectroscopy. *J. Phys. Chem. B* **2013**, *117*, 4733–4739.

23 Cai, Q.; Kusnetzow, A. K.; Hideg, K.; Price, E. A.; Haworth, I. S.; Qin, P. Z. Nanometer distance measurements in RNA using site-directed spin labeling. *Biophys. J.* **2007**, *93*, 2110–2117.

24 Malkin, R.; Bearden, A. J. Primary reactions of photosynthesis: photoreduction of a bound chloroplast ferredoxin at low temperature as detected by EPR spectroscopy. *Proc. Natl. Acad. Sci. U.S.A.* **1971**, *68*, 16–19.

25 Bolton, J. R.; Cammack, R. Primary electron acceptor complex of photosystem I in spinach chloroplasts. *Nature* **1975**, *256*, 668–670.

26 Rouault, T. A.; Stout, C. D.; Kapatin, S.; Harford, J. B.; Klausner, R. D. Structural relationship between an iron-regulated RNA-binding protein (IRE-BP) and aconitase: functional implications. *Cell* **1991**, *64*, 881–883.

27 Hentze, M. W.; Argos, P. Homology between IRE-BP, a regulatory RNA-binding protein, aconitase, and isopropylmalate isomerase. *Nucleic Acids Res.* **1991**, *19*, 1739–1740.

28 Enemark, J. H.; Young, C. G. Bioinorganic chemistry of protein-containing molybdenum and tungsten enzymes. *Adv. Inorg. Chem.* **1993**, *40*, 1–88.

29 Reczkowski, R. S.; Ash, D. E. EPR evidence for binuclear manganese(II) centers in rat liver arginase. *J. Am. Chem. Soc.* **1992**, *114*, 10992–10994.

30 Khangulov, S. V.; Pessiki, P. J.; Barynin, V. V.; Ash, D. E.; Dismukes, G. C. Determination of the metal ion separation and energies of the three lowest electronic states of dimanganese(II,II) complexes and enzymes: Catalase and liver Arginase. *Biochemistry* **1995**, *34*, 2015–2025.

31 Shi, O.; Morris, S. M., Jr.; Zoghbi, H.; Porter, C. W.; O'Brien, W. E. Generation of a mouse model for Arginase II deficiency by targeted disruption of the arginase II gene. *Mol. Cell. Biol.* **2001**, *21*, 811–813.

32 Lovell, M. A.; Robertson, J. D.; Teesdale, W. J.; Campbell, J. L.; Markesbery, W. R. Copper, iron and zinc in Alzheimer's disease senile plaques. *J. Neurol. Sci.* **1998**, *158*, 47–52.

33 Huang, X.; Cuajungco, M.; Atwood, C. G.; Hartshorn, M. A.; Tyndall, J. D. A.; Hanson, G. R.; Stokes, K. C.; Leopold, M.; Multhaup, G.; Goldstein, L. E.; Scarpa, R. C.; Saunders, A. J.; Lom, J.; Moir, R. D.; Glabe, C.; Bowden, E. F.; Masters, C. L.; Fairlie, D. P.; Tanzi, R. E.; Bush, A. I. Cu(II) potentiation of Alzhermer Aβ neurotoxicity. *J. Biol. Chem.* **1999**, *274*, 37111–37116.

34 Bush, A. I. Metal complexing agents and therapies for Alzheimer's disease. *Neurobiol. Aging* **2002**, *23*, 1031–1038.

35 Kirkitadze, M. D.; Bitan, G.; Teplow, D. B. Paradigm shifts in Alzhermer's disease and other neurodegenerative disorders: The emerging role of oligomeric assemblies. *J. Neurosci. Res.* **2002**, *69*, 567–577.

36 Miller, L. M.; Wang, Q.; Telivala, T. P.; Smith, R. J.; Lanzirotti, A.; Miklossy, J. Synchrotron-based infrared and X-ray imaging shows focalized accumulation of Cu and Zn co-localized with β-amyloid deposits in Alzheimer's disease. *J. Struct. Biol.* **2006**, *155*, 30–37.

37 Waldron, K. J.; Rutherford, J. C.; Ford, D.; Robinson, N. J. Metalloproteins and metal sensing. *Nature* **2009**, *460*, 823–830.

38 van Amsterdam, I. M. C.; Ubbink, M.; Canters, G. W.; Huber, M. Measurement of a Cu-Cu distance of 26 A by a pulsed EPR method. *Angew. Chem., Int. Ed.* **2003**, *42*, 62–64.

39 Narr, E.; Godt, A.; Jeschke, G. Selective measurements of a nitroxide-nitroxide separation of 5 nm and a nitroxide-copper separation of 2.5 nm in a terpyridine-based copper(II) complex by pulse EPR spectroscopy. *Angew. Chem., Int. Ed.* **2002**, *41*, 3907–3910.

40 Kay, C. W. M.; Mkami, H. E.; Cammack, R.; Evans, R. W. Pulsed ELDOR determination of the intramolecular distance between the metal binding sites in dicupric human serum transferrin and lactoferrin. *J. Am. Chem. Soc.* **2007**, *129*, 4868–4869.

41 Bode, B. E.; Plackmeyer, J.; Prisner, T. F.; Schiemann, O. PELDOR measurements on a nitroxide-labeled Cu(II) porphyrin: Orientation selection, spin-density distribution, and conformational flexibility. *J. Phys. Chem. A* **2008**, *112*, 5064–5073.

42 Bode, B. E.; Plackmeyer, J.; Bolte, M.; Prisner, T. F.; Schiemann, O. PELDOR on an exchange coupled nitroxide copper(II) spin pair. *J. Organomet. Chem.* **2009**, *694*, 1172–1179.

43 Yang, Z.; Kise, D.; Saxena, S. An approach towards the measurement of nanometer range distances based on Cu^{2+} ions and ESR. *J. Phys. Chem. B* **2010**, *114*, 6165–6174.

44 Yang, Z.; Kurpiewski, M. R.; Ji, M.; Townsend, J. E.; Mehta, P.; Jen-Jacobson, L.; Saxena, S. ESR spectroscopy identifies inhibitory Cu^{2+} sites in a DNA-modifying enzyme to reveal determinants of catalytic specificity. *Proc. Natl. Acad. Sci. U.S.A.* **2012**, *109*, E993–E1000.

45 Elsaesser, C.; Brecht, M.; Bittl, R. Pulsed electron-electron double resonance on multinuclear metal clusters: Assignment of spin projection factors based on the dipolar interaction. *J. Am. Chem. Soc.* **2002**, *124*, 12606–12611.

46 Elsaesser, C.; Brecht, M.; Bittl, R. Treatment of spin-coupled metal centres in pulsed electron-electron double-resonance experiments. *Biochem. Soc. Trans.* **2005**, *33*, 15–19.

47 Roessler, M. M.; King, M. S.; Robinson, A. J.; Armstrong, F. A.; Harmer, J.; Hirst, J. Direct assignment of EPR spectra to structurally defined iron-sulfur clusters in complex I by double electron−electron resonance. *Proc. Natl. Acad. Sci. U.S.A.* **2010**, *107*, 1930–1935.

48 Raitsimring, A. M.; Gunanathan, C.; Potapov, A.; Efremenko, I.; Martin, J. M.; Milstein, D.; Goldfarb, D. Gd^{3+} complexes as potential spin labels for high field pulsed EPR distance measurements. *J. Am. Chem. Soc.* **2007**, *129*, 14138–14139.

49 Lueders, P.; Jeschke, G.; Yulikov, M. Double electron-electron resonance measured between Gd^{3+} ions and nitroxide radicals. *J. Phys. Chem. Lett.* **2011**, *2*, 604–609.

50 Kaminker, I.; Yagi, H.; Huber, T.; Feintuch, A.; Otting, G.; Goldfarb, D. Spectroscopic selection of distance measurements in a protein dimer with mixed nitroxide and Gd^{3+} spin labels. *Phys. Chem. Chem. Phys.* **2012**, *14*, 4355–4358.

51 Potapov, A.; Yagi, H.; Huber, T.; Jergic, S.; Dixon, N. E.; Otting, G.; Goldfarb, D. Nanometer-scale distance measurements in proteins using Gd^{3+} spin labeling. *J. Am. Chem. Soc.* **2010**, *132*, 9040–9048.

52 Song, Y.; Meade, T. J.; Astashkin, A. V.; Klein, E. L.; Enemark, J. H.; Raitsimring, A. Pulsed dipolar spectroscopy distance measurements in biomacromolecules labeled with Gd(III) markers. *J. Magn. Reson.* **2011**, *210*, 59–68.

53 Potapov, A.; Song, Y.; Meade, T. J.; Goldfarb, D.; Astashkin, A. V.; Raitsimring, A. Distance measurements in model bis-Gd(III) complexes with flexible "bridge". Emulation of biological molecules having flexible structure with Gd(III) labels attached. *J. Magn. Reson.* **2010**, *205*, 38–49.

54 Yagi, H.; Banerjee, D.; Graham, B.; Huber, T.; Goldfarb, D.; Otting, G. Gadolinium tagging for high-precision measurements of 6 nm distances in protein assemblies by EPR. *J. Am. Chem. Soc.* **2011**, *133*, 10418–10421.

55 Kaminker, I.; Tkach, I.; Manukovsky, N.; Huber, T.; Yagi, H.; Otting, G.; Bennati, M.; Goldfarb, D. W-band orientation selective DEER measurements on a Gd^{3+}/nitroxide mixed-labeled protein dimer with a dual mode cavity. *J. Magn. Reson.* **2013**, *227*, 66–71.

56 Yulikov, M.; Lueders, P.; Warsi, M. F.; Chechik, V.; Jeschke, G. Distance measurements in Au nanoparticles functionalized with nitroxide radicals and Gd^{3+}−DTPA chelate complexes. *Phys. Chem. Chem. Phys.* **2012**, *14*, 10732–10746.

57 Matalon, E.; Huber, T.; Hagelueken, G.; Graham, B.; Frydman, V.; Feintuch, A.; Otting, G.; Goldfarb, D. Gadolinium(III) spin labels for high-sensitivity distance measurements in transmembrane helices. *Angew. Chem., Int. Ed. Engl.* **2013**, *52*, 1–5.

58 Banerjee, D.; Yagi, H.; Huber, T.; Otting, G.; Goldfarb, D. Nanometer-range distance measurement in a protein using Mn^{2+} tags. *J. Phys. Chem. Lett.* **2012**, *3*, 157–160.

59 Goldfarb, D. *Metal-Based Spin Labeling for Distance Determination*; Springer: Berlin Heidelberg, 2012.

60 Stone, K.; Townsend, J. E.; Sarver, J.; Sapienza, P. J.; Saxena, S.; Jen-Jacobson, L. Electron spin resonance shows common structural features for different classes of EcoRI-DNA complexes. *Angew. Chem., Int. Ed.* **2008**, *47*, 10192–10194.

61 Maryasov, A. G.; Tsvetkov, Y. D.; Raap, J. Weakly coupled radical pairs in solids: ELDOR in ESE structure studies. *Appl. Magn. Reson.* **1998**, *14*, 101–113.

62 Milov, A. D.; Tsvetkov, Y. D.; Formaggio, F.; Crisma, M.; Toniolo, C.; Raap, J. The secondary structure of a membrane-modifying peptide in a supramolecular assembly studied by PELDOR and CW-ESR spectroscopies. *J. Am. Chem. Soc.* **2001**, *123*, 3784–3789.

63 Salikhov, K. M.; Dzuba, S. A.; Raitsimring, A. M. The theory of electron spin-echo signal decay resulting from dipole-dipole interactions between paramagnetic centers in solids. *J. Magn. Reson.* **1981**, *42*, 255–276.

64 Jeschke, G.; Polyhach, Y. Distance measurements on spin-labelled biomacromolecules by pulsed electron paramagnetic resonance. *Phys. Chem. Chem. Phys.* **2007**, *9*, 1895–1910.

65 Yang, Z.; Ji, M.; Saxena, S. Practical aspects of copper-ion based DEER distance measurements. *Appl. Magn. Reson.* **2010**, *39*, 487–500.

66 Ruthstein, S.; Ji, M.; Mehta, P.; Jen-Jacobson, L.; Saxena, S. Sensitive Cu^{2+}-Cu^{2+} distance measurements in a protein-DNA complex by DQC-ESR. *J. Phys. Chem. B* **2013**, *117*, 6227–6230.

67 Yang, Z.; Becker, J.; Saxena, S. On Cu(II)−Cu(II) distance measurements using pulsed electron electron double resonance. *J. Magn. Reson.* **2007**, *188*, 337–343.

68 Lovett, J. E.; Bowen, A. M.; Timmel, C. R.; Jones, M. W.; Dilworth, J. R.; Caprotti, D.; Bell, S. G.; Wong, L. L.; Harmer, J. Structural information from orientationally selective DEER spectroscopy. *Phys. Chem. Chem. Phys.* **2009**, *11*, 6840–6848.

69 Godt, A.; Schulte, M.; Zimmermann, H.; Jeschke, G. How flexible are poly(paraphenyleneethynylene)s? *Angew. Chem., Int. Ed.* **2006**, *45*, 7560–7564.

70 Kaminker, I.; Florent, M.; Epel, B.; Goldfarb, D. Simultaneous acquisition of pulse EPR orientation selective spectra. *J. Magn. Reson.* **2011**, *208*, 95–102.

71 Marko, A.; Margraf, D.; Yu, H.; Mu, Y.; Stock, G.; Prisner, T. F. Molecular orientation studies by pulsed electron-electron double resonance experiments. *J. Chem. Phys.* **2009**, *130*, No. 064102.

72 Woodhead, J. L.; Bhave, N.; Malcolm, A. D. B. Cation dependence of restriction endonuclease EcoRI activity. *Eur. J. Biochem.* **1981**, *115*, 293–296.

73 Grigorescu, A.; Horvath, M.; Wilkosz, P.; Chandrasekhar, K.; Rosenberg, J. In *Restriction Endonucleases*; Springer-Verlag: Heidelberg, 2004; pp 137−177.

74 Kurpiewski, M. R.; Engler, L. E.; Wozniak, L. A.; Kobylanska, A.; Koziolkiewicz, M.; Stec, W. J.; Jen-Jacobson, L. Mechanism of coupling between DNA recognition specificity and catalysis in EcoRI endonuclease. *Structure* **2004**, *12*, 1775–1788.

75 van Wonderen, J.; Kostrz, D. N.; Dennison, C.; MacMillan, F. Refined distances between paramagnetic centers of a multi-copper nitrite reductase determined by pulsed EPR (iDEER) spectroscopy. *Angew. Chem., Int. Ed.* **2013**, *52*, 1990–1993.

76 Jeschke, G.; Chechik, V.; Ionita, P.; Godt, A.; Zimmermann, H.; Banham, J.; Timmel, C. R.; Hilger, D.; Jung, H. DeerAnalysis2006—a comprehensive software package for analyzing pulsed ELDOR data. *Appl. Magn. Reson.* **2006**, *30*, 473–498.

77 Sengupta, I.; Nadaud, P. S.; Jaroniec, C. P. Protein structure determination with paramagnetic solid-state NMR spectroscopy. *Acc. Chem. Res.* **2013**, *46*, 2117–2126.